processes

MDPI

Article

Simultaneous Monitoring of the Effects of Multiple Ionic Strengths on Properties of Copolymeric Polyelectrolytes during Their Synthesis

Aide Wu [1], Zifu Zhu [1], Michael F. Drenski [2] and Wayne F. Reed [1,*]

[1] Physics Dept., Tulane University, New Orleans, LA 70115, USA; awu2@tulane.edu (A.W.); zzhu@tulane.edu (Z.Z.)

[2] Advanced Polymer Monitoring Technologies, Inc., 1078 S. Gayoso St., New Orleans, LA 70125, USA; mdrenski@tulane.edu

* Correspondence: wreed@tulane.edu; Tel.: +1-504-862-3185

Academic Editor: Alexander Penlidis

Received: 20 February 2017; Accepted: 7 April 2017; Published: 11 April 2017

Abstract: A new Automatic Continuous Online Monitoring of Polymerization reactions (ACOMP) system has been developed with multiple light scattering and viscosity detection stages in serial flow, where solution conditions are different at each stage. Solution conditions can include ionic strength (IS), pH, surfactants, concentration, and other factors. This allows behavior of a polymer under simultaneous, varying solution conditions to be monitored at each instant of its synthesis. The system can potentially be used for realtime formulation, where a solution formulation is built up additively in successive stages. It can also monitor the effect of solution conditions on stimuli responsive polymers, as their responsiveness changes during synthesis. In this first work, the new ACOMP system monitored light scattering and reduced viscosity properties of copolymeric polyelectrolytes under various IS during synthesis. Aqueous copolymerization of acrylamide (Am) and styrene sulfonate (SS) was used. Polyelectrolytes in solution expand as IS decreases, leading to increased intrinsic viscosity (η) and suppression of light scattering intensity due to electrostatically enhanced second and third virial coefficients, A_2 and A_3. At a fixed IS, the same effects occur if polyelectrolyte linear charge density (ξ) increases. This work presents polyelectrolyte response to a series of IS and changing ξ, during chemical synthesis.

Keywords: ACOMP; online monitoring; copolymeric polyelectrolytes; light scattering; viscosity

1. Background and Motivation

This work introduces a new version of the Automatic Continuous Online Monitoring of Polymerization reactions (ACOMP) system ("second generation ACOMP") whose aim is to monitor the onset and evolution of stimuli responsive behavior, under multiple simultaneous solution conditions, during the synthesis of stimuli responsive polymers (SRP). SRP is a vast area of modern polymer science and engineering, aimed at producing polymers that can respond to such stimuli as temperature, radiation, and solution conditions such as pH, ionic strength, polymer concentration, presence of such agents as surfactants, nanoparticles, hydrophobic species, etc. The types of responses that can occur in response to these stimuli include coil/globule phase transitions, polymer coil expansion or shrinkage, micellization, aggregation, and other forms of spontaneous self-assembly.

These next-generation materials are expected to have applications in medicine, sensors, self-healing materials, and environmental remediation [1–5]. Hydrogels ofpoly(*N*-isopropylacrylamide), for example, have a lower critical solution temperature (LCST), near body temperature, which makes it a candidate for drug delivery applications in which the NIPAM-based polymer releases its medical

payload when in contact with targeted tissues [6,7]. While SRP hold much promise, their synthesis is complex and must be tightly controlled. For example, self-assembly of SRP block copolymers into well-defined nanostructures occurs only over a narrow range of compositions, and this ability can be lost with errors in composition as low as two to five percent [8].

A major reason for the development of Second Generation ACOMP (SGA) is to not only monitor synthesis and the onset and evolution of stimuli responsiveness, but also to control the synthetic reactions. Much work in SRP research makes use of controlled radical and other living type reactions [9–14] nucleobase polymers [15,16], and information containing polymers [17,18].

1.1. Background on Solution Properties of Polyelectrolytes in Solution

In this first work with the new version of ACOMP a stimuli responsive copolymer produced by simple free radical copolymerization was chosen, rather than the more sophisticated living-type, "click", postpolymer modifications and other routes under current research for producing stimuli responsive polymers.

While the physical properties of polyelectrolytes in solution still present some surprises and puzzles, certain general principles are well established, both experimentally and theoretically. For example, it is well known that the free energy of linear polyelectrolytes in solution is composed of an enthalpic term that expands the polymer coil due to mutual electrostatic repulsion among charge groups, and an entropic term that contracts the coil towards higher probability conformations. The net effect of the free energy balance is a polymer coil that is expanded with respect to a neutral polymer of otherwise identical properties. As the ionic strength of the supporting solution increases, the electrostatic repulsion among charges in the chain decreases and the coil shrinks, which can be measured in many ways, such as by a decrease in polymer reduced viscosity or by an increase in light scattering intensity due to decreased interchain repulsion and excluded volume, and correspondingly reduced second and third virial coefficients A_2 and A_3, respectively. Similarly, if the linear charge density (ξ) is increased at a fixed IS the coil will also expand. ξ can be changed by altering pH for a polybase or polyacid.

Persistence length is a central notion in the theory of polymer conformations and has been examined in detail [19]. The complex problem of excluded volume for polymers has likewise undergone extensive examination [20–23]. The details of the free energy and corresponding calculations of electrostatically enhanced excluded volume and persistence lengths have been treated theoretically and experimentally [24–27]. Similarly, the theory of counterion condensation has been developed and demonstrated experimentally [28–31]. In its simplest statement, counterion condensation predicts that when the repulsive electrostatic energy between charge groups on a polymer chain exceeds thermal energy k_BT (where k_B is Boltzmann's constant), counterions will condense along the chain to lower linear charge density ξ, until the repulsive energy is less than or equal to k_BT. A recent ACOMP application succeeded in monitoring the cross-over from counterion condensation to non-condensation regimes during copolymer synthesis of anionic and neutral comonomers [32]. In this latter work the authors introduced the term "copolyelectrolyte" as an abbreviation for "copolymer polyelectrolyte".

The current work deals with synthesis of copolyelectrolytes composed of neutral acrylamide (Am) and anionic styrene sulfonate (SS). The reactivity ratios introduced by Mayo and Lewis provide a convenient means of assessing mutual reactivity of comonomers [33]. Given two comonomers, A and B, the reactivity ratio r_A is the ratio of the probability that A will react with another A upon encounter to the probability that A will react with B upon encounter. The reactivity ratio r_B is defined similarly for comonomer B. If r_A and r_B are each zero, then a strictly alternating copolymer will be formed. If r_A and r_B are each infinite, then only homopolymers of A and of B will be produced when the two polymerize in the same reactor. If $r_A = r_B = 1$ then a statistical copolymer is formed whose instantaneous composition only depends on the molar concentrations of A and B, and their respective free radicals, at that instant.

The following approximate values were found using ACOMP for acrylamide and styrene sulfonate copolymerization; $r_{Am} = 0.18$, $r_{SS} = 2.14$ [34]. Since $r_{SS} >> r_{Am}$ it is expected that chains formed early in the copolymerization will be rich in SS, and hence be highly charged. Furthermore, the SS should be consumed rapidly, leaving Am to homopolymerize later in the reaction, after the SS is used up. These trends are clearly seen in ACOMP data.

1.2. Background on ACOMP

ACOMP was first introduced in 1998 [35] and was recently reviewed in detail [36]. It has been used in many scenarios including free radical copolymerization [37,38], copolyelectolytes [39], branching reactions [40], emulsion [41] and inverse emulsion [42] reactions, in batch, semi-batch [43] and continuous reactors [44], for aqueous and organic solvents, for post-polymerization and derivitization reactions [45], and for the controlled radical polymerization routes nitroxide-mediated polymerization (NMP) [46], atom transfer radical polymerization (ATRP) [47], reversible addition fragmentation transfer polymerization (RAFT) [48], and ring opening metathesis polymerization (ROMP) [49]. Simultaneous monitoring of both polymer reaction characteristics and colloid size distributions (latex and monomer droplets) was also achieved in emulsion polymerization [41]. Recently, fully automatic feedback control of free radical polymerization was achieved [50]. The first system controlled was aqueous polymerization of Am. Current work includes simultaneous automatic feedback control of composition and molecular weight during free radical copolymerization, automatic production of multi-modal polymers, and extension of control to living type polymerization. The work presented here is cognate to the latter effort.

ACOMP relies on the continuous extraction, dilution, and conditioning of a small sample stream from the reactor on which measurements by various combinations of detectors are made. By combining simultaneous data from multiple detectors continuous monitoring of salient reaction characteristics can be made, such as kinetics, conversion of comonomers, composition drift, evolution of molecular mass and intrinsic viscosity, and detection of unusual phenomena, such as microgelation and runaway reactions. Typical detectors include light scattering, UV/visible spectrophotometry, viscometry, refractivity, and polarimetry. While ACOMP is not inherently a chromatographic method, its continuous stream can be used in automatic conjunction with gel permeation and other separation techniques, as has been demonstrated [51].

2. Second Generation ACOMP (SGA) for Monitoring the Synthesis of Stimuli Responsive Polymers under Varying Solution Conditions

The aims of this work are (1) to introduce the multi-stage serial flow SGA; (2) apply it to the monitoring of copolyelectrolyte synthesis in batch; (3) to qualitatively interpret the results within well understood concepts of polyelectrolyte behavior. It is beyond the scope of this work to develop a complete theoretical formulation for interpreting all the data, such as by electrostatic persistence length, excluded volume theory, and counterion condensation theories.

An earlier version of SGA allowed control of temperature in three detection stages, each stage with a light scattering and viscometer. This was used to study the effects on the lower critical solution temperature (LCST) of copolymerizing n-isopropyl acrylamide (NIPAM) with more hydrophilic comonomers [52,53].

In this work the custom built SGA comprises (i) a system of pumps and a high pressure and a low pressure mixing chamber for continuously withdrawing and diluting reactor content at a low flow rate, typically 0.1 mL/min; (ii) up to seven detector stages in series, each with a custom built single capillary viscometer and a 90° custom built light scattering flow cell; (iii) a high pressure multi-head syringe pump that feeds concentrated NaCl solutions into each stage, thus increasing ionic strength (IS) from stage to stage; (iv) A separate, highly dilute stream at 150 mM NaCl from the low pressure mixing chamber is fed to a diode array UV spectrophotometer, covering the range 190–400 nm (Shimadzu SPD-M20A). From the UV detector, the stream flows through a seven angle light scattering unit

(BI-MwA from Brookhaven Instruments Corp., New York, NY, USA); (v) Data from all the detectors are collected under various protocols and unified in realtime into a master file to allow cross-correlations and calculations using the different signals.

Hence, the SGA combines (i) the features of the original ACOMP to monitor copolymer weight average molecular weight and reduced viscosity, and cumulative and instantaneous copolymer composition with (ii) the ability to interrogate the polymer continuously during synthesis as to its light scattering and viscometric responses to a series of IS.

The SGA system is equipped with two Nexus 6000 high pressure syringe pumps (By Chemyx Inc., Stafford, TX, USA) which infuse NaCl solutions with different concentrations in each syringe into the serial flow, in order to change the ionic strength at each stage. To meet the operation/characterization under high pressure operation condition, stainless steel syringes (Harvard Apparatus, MA, USA) are used to hold the NaCl solutions for injection into the serial flow. The sample extraction and dilution system consists of four Shimadzu AD-VP HPLC pumps. A system diagram is shown in Scheme 1. Pump 1 extracts sample directly from the reactor, Pump 2 and Pump 3 are used for diluting sample with deionized water as a first dilution. A separate HPLC pump delivers this first stage dilution stream through the multi-stage serial dilution stage with the LS/viscometer detection pairs, where the IS is increased at each stage via the syringe pumps. A second dilution of the first stream occurs in a second high pressure mixing chamber producing a highly dilute sample at 150 mM IS, which is sent to a detection stage comprising a UV-vis (Shimadzu SPD-M20A, Kyoto, Japan) and BI-MwA (Brookhaven Instruments Corporation, New York, NY, USA). This highly dilute stream at 150 mM IS allows determination of M_w without interference from the large virial coefficient effects deliberately produced in the more highly concentrated, multi-stage IS detector train. All detectors were at room temperature.

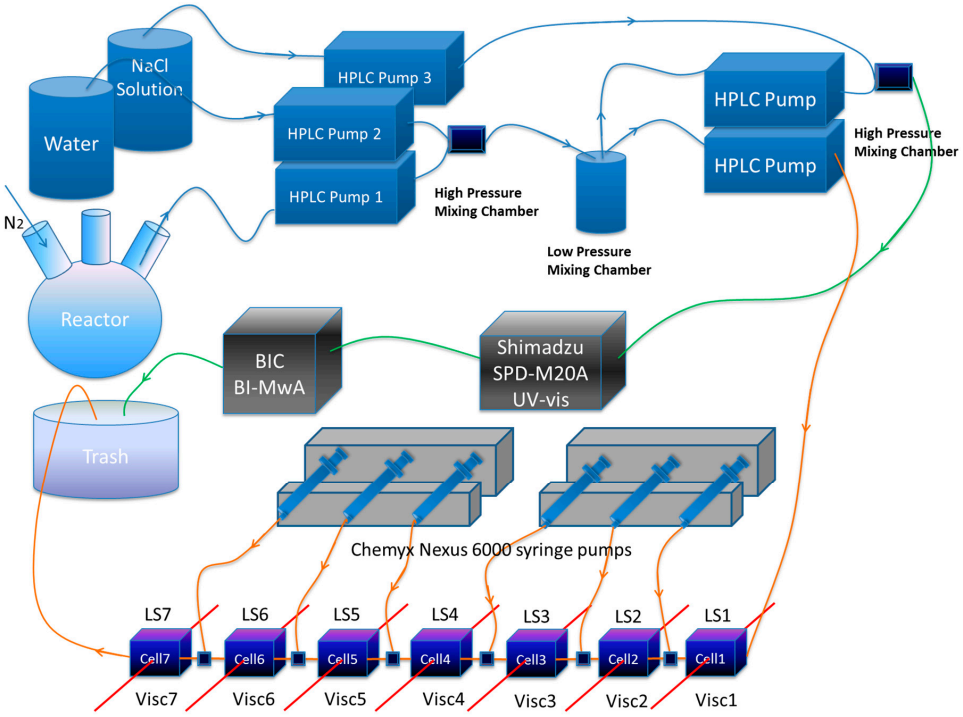

Scheme 1. The Second Generation Automatic Continuous Online Monitoring of Polymerization reactions (SGA) instrumentation.

Table 1 provides information on each reaction, including the amount of dilution in the first and second dilution stages. Table 2 shows the syringe pump reservoir strength of each stage, the IS of the serial flow at each stage, and the additional, small dilution that occurs in each stage.

Table 1. The information for each of the three reactions.

Reaction	Type	Am_0 (g/cm^3)	SS_o (g/cm^3)	Initiator (g/cm^3)	Second Dilution	First Dilution	T (°C)	Figures
A	50/50 batch	12.9×10^{-3}	37.5×10^{-3}	2.73×10^{-3}	50×	10×	65	Figure 1a,b, Figure 2, Figure 3, Figure 7a
B	50/50 batch	10.3×10^{-3}	32.5×10^{-3}	5.00×10^{-4}	105×	15×	60	Figure 4a,b, Figure 5, Figure 6
C	Semi-batch	18.1×10^{-3}	181×10^{-3} stock fed into reactor at 0.1 mL/min	2.73×10^{-3}	50×	10×	65	Figure 7b

Table 2. The flow rates, dilution factors, and ionic strengths in the seven stage SGA detector train.

	Reaction A			Reaction B			Reaction C (Semi-Batch)		
Stage	[NaCl] * (mM)	IS (mM)	Dilution factor	[NaCl] * (mM)	IS (mM)	Dilution factor	[NaCl] * (mM)	IS (mM)	Dilution factor
1	0	0	1	0	0	1	0	0	1
2	2	0.095	1.05	4	0.12	1.03125	2	0.095	1.05
3	20	1	1.10	40	1.3	1.0625	20	1	1.10
4	200	9.7	1.15	400	13	1.09375	200	9.7	1.15
5	1000	51	1.20	5000	151	1.125	1000	51	1.20
6	2000	129	1.25	-	-	-	2000	129	1.25
7	5000	316	1.30	-	-	-	5000	316	1.30

* Ionic strength (IS) of reservoir.

Viscosity computations are based on Poisseuille flow of a liquid of viscosity η in a capillary of length L and radius R at a flow rate Q (cm^3/s), for which the pressure drop ΔP across the capillary is

$$\Delta P = \frac{8LQ\eta}{\pi R^4} \tag{1}$$

The dilute solution polynomial expansion for viscosity is used to interpret the viscometer data:

$$\eta = \eta_s \left[1 + [\eta]c + k_p[\eta]^2 c^2\right] \tag{2}$$

where η_s is the pure solvent viscosity, [η] is the intrinsic viscosity of the polymer, C_p is the polymer concentration (in g/cm^3) and k_H is a constant related to the hydrodynamic interactions between polymer chains, usually around 0.4 for neutral, coil polymers [54]. The intrinsic viscosity is the extrapolation to zero concentration and zero shear rate of the reduced viscosity η_r, which is defined according to Equation (2) by

$$\eta_r(t) = \frac{\eta(t) - \eta_s}{\eta_s C_p} = \frac{V(t) - V_s}{(V_s - V_0)C_p} \tag{3}$$

In the second equality $V(t)$ is the time dependent viscometer signal, V_s is the voltage of the pure solvent baseline, and V_0 accounts for any voltage offset in the viscometer when the flow rate through it is Q = 0. This latter can be written as shown because the viscometer voltage output is directly proportional to ΔP. It is important to realize that because the denominator divides out by solvent baseline voltage, no calibration factor for the capillary viscometer is needed in order to determine η_r. The specific viscosity η_{sp} is another useful quantity computed by

$$\eta_{sp}(t) = \frac{\eta(t) - \eta_s}{\eta_s} = \frac{V(t) - V_s}{V_s - V_o} \tag{4}$$

The absolute excess Rayleigh ratio is determined from the raw light scattering voltages by

$$I_R(t) = \frac{V(t) - V_s}{V_s - V_d} I_{R,toluene} \tag{5}$$

where $V(t)$ is the scattering from the polymer solutions, V_s is the scattering from the pure solvent and V_d is the dark voltage of the detector when there is no incident light on the scattering sample. $I_{R,toluene}$ is the Rayleigh ratio for pure toluene at T = 25 °C, which is given for any wavelength by

$$I_R(\mathrm{cm}^{-1}) = 1.069 \times 10^{-5} \left(\frac{677}{\lambda(\mathrm{nm})} \right)^4 \tag{6}$$

I_R measures the fraction of incident light scattered per cm of path through the scattering medium. I_R is used for light scattering analysis using the usual Zimm approach [55]:

$$\frac{Kc}{I_R(q, C_p)} = \frac{1}{MP(q)} + 2A_2C_p + \left[3A_3Q(q) - 4{A_2}^2MP(q)(1 - P(q))\right]C_p + ...^2 \tag{7}$$

where K is an optical constant, given for vertically polarized incident light by

$$K = \frac{4\pi^2 n^2 (dn/dc)^2}{N_A \lambda^4} \tag{8}$$

where n is the solvent index of refraction, λ is the vacuum wavelength of the incident light, dn/dc is the differential refractive index for the polymer in the chosen solvent, and q is the usual scattering wave-vector amplitude, $q = (4\pi n/\lambda)\sin(\theta/2)$, where θ is the scattering angle.

In the limit as $q \to 0$, and for polydisperse polymers this reduces to

$$\frac{KC_p}{I_R(q = 0, C_p)} = \frac{1}{M_w} + 2A_2C_p + 3A_3{C_p}^2 + ... \tag{9}$$

where M_w is the weigh average molecular weight and A_2 and A_3 are complex averages of the virial coefficients.

The individually resolved concentrations of Am and SS can be used to compute the instantaneous mole fractions of Am and SS in a copolymer at any instant according to

$$[\mathrm{F}_{\mathrm{inst,Am}}] = \frac{d[\mathrm{Am}]}{d([\mathrm{Am}] + [\mathrm{SS}])} \tag{10a}$$

$$[F_{inst,SS}] = \frac{d[SS]}{d([Am] + [SS])} \tag{10b}$$

3. Copolymerization

Sodium 4-vinylbenzenesulfonate and acrylamide were used as received from Sigma-Aldrich. The initiator, 2,2′-azobis(2-amidinopropane dihydrochloride (V-50), was from Wako Chemicals USA, Inc. For batch reactions A and B comonomers with molar ratio of 1:1 were fully dissolved in DI water, and the reactions were carried out in a thermostated three neck reactor under continuous N_2 purge. The starting comonomers' concentrations and reaction temperatures are listed in Table 1 for Reactions A, B, and C. Linear charge density ξ, varies during synthesis due to the high composition drift of the copolymeric system; anionic styrene sulfonate (SS) and electrically neutral acrylamide (Am), which have widely separated reactivity ratios (r_{Am} = 0.18, r_{SS} = 2.14 in 0.1 M NaCl [39], and with similar high drift at other ionic strengths). The salt, the sodium form of styrene sulfonate remains ionized at the near-neutral pH of the reactor solution. There was no added NaCl in the reactor.

Although a salt is used here (SS) the use of the acid form, sulfonic acid, could lead to different behavior in the polymer, beyond the counterion condensation effect expected even for salts, since pK_a for acids and bases in polymers is different than in their small molecule form. ACOMP has previously used both pH and conductivity probes in the reactor to follow changes in these quantities and would normally be used in such cases.

4. Results and Discussion

4.1. Typical Raw Data

Figure 1a shows typical raw data for a 50/50 VB/Am copolymerization, where η_{sp} and I_R are computed by Equations (4) and (5), respectively. The conditions are given in Table 1. The reaction began at 8000 s. The time scale of the reaction corresponds to earlier findings [39]. Only three IS of the seven measured are shown, in order to keep the figure legible. The trend for viscosity is as expected, namely as IS increases there is a dramatic drop in η_{sp} at any given instant, reflecting coil contraction as charges are electrostatically shielded. The light scattering (LS) at low IS, 0.1 mM, is highly suppressed. Also a maximum is reached as the reaction proceeds follow by a steady drop and subsequent small rise late in the reaction, starting at about 16,000 s. The maximum is due to the effect of A_3, seen in Equation (9), as the concentration builds. A similar shape and effect is seen at 10 mM, except the overall magnitude of the LS is well above that for 0.1 mM, due to significantly reduced A_2 and A_3. At 130 mM the A_3 effect is completely suppressed and LS increases monotonically as the reaction proceeds. At 130 mM the solution is about 10% more dilute than at 10 mM. The slight rise in LS for 0.1 mM starting at 16,000 s, is also seen for 10 mM and 130 mM LS. This is due to the fact that the high reactivity ratio of SS leads to its complete consumption at about 16,000 s, leaving only Am, which produces more massive homopolymer chains than the copolymer chains. The trend can also be seen in the viscosity data, although less pronounced.

Figure 1b shows the total fractional polymer conversion f_{total}, and the instantaneous molar fractions of Am and SS in copolymers produced at a given instant, $[F_{inst,Am}]$ and $[F_{inst,SS}]$, according to Equations (10a,b). This shows that SS is consumed more rapidly, due to its higher reactivity ratio, leaving chains with decreasing fraction of SS as the reaction progresses.

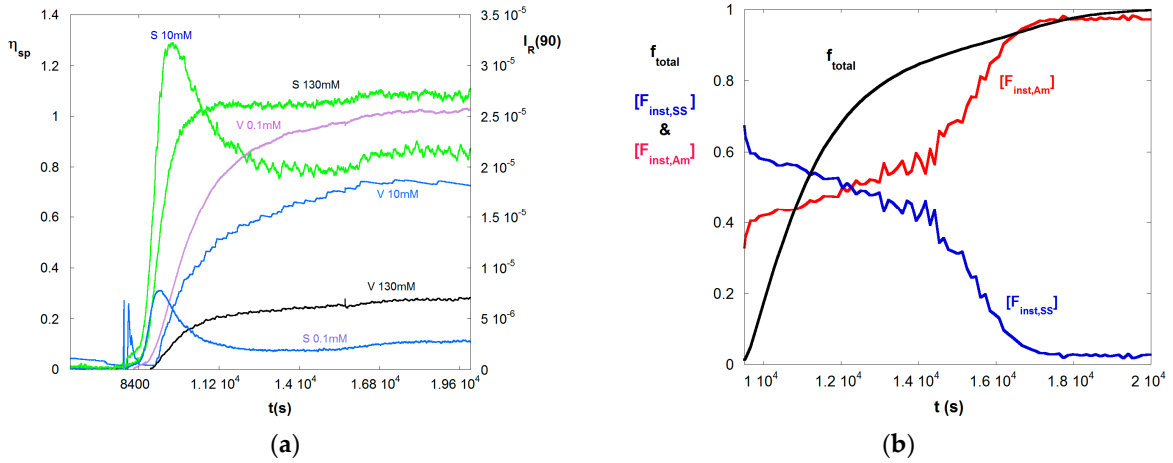

(**a**) (**b**)

Figure 1. (**a**) A selection of LS (S) and η_{sp} (V) data for 50/50 *M*/*M* copolymerization of Am and SS shown at three of the seven different IS available; 0.1 mM, 10 mM, and 130 mM for reaction A; (**b**) Total monomer conversion f_{total}, and instantaneous mole fractions $F_{inst,Am}$, and $F_{inst,SS}$ for reaction A.

4.2. SGA Data Analysis

Figure 2 shows Kc/I_R vs. C_p for Reaction A up to 15,000 s. C_p is the polymer concentration in the detector train. Also shown are quadratic fits, which yield A_2, and A_3 for each, according to

Equation (9). In these fits M_w was determined by linear extrapolation at low C_p to be 67,000 g/mol ±5% and showed low drift through the early and mid-stages of the reaction. It was held constant in the quadratic fit, leaving A_2 and A_3 as the fit variables. Figure 3 shows these latter values obtained from the quadratic fits.

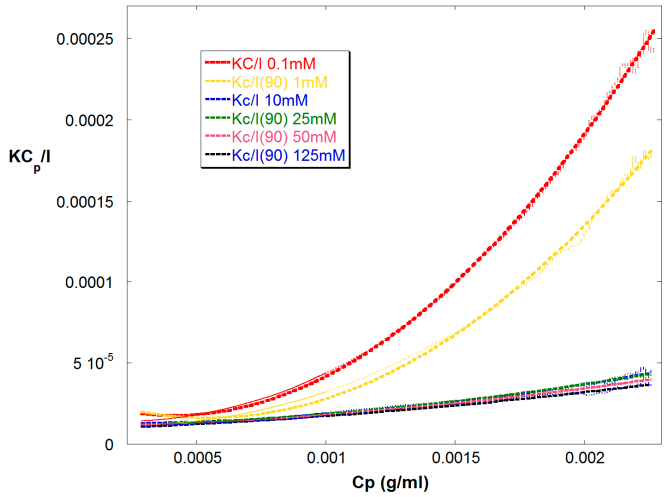

Figure 2. $KC_p/I_R(90)$ vs. C_p for reaction A, where C_p is the total polymer concentration in the detector train. Also shown are quadratic fits for A_2 and A_3 with fixed M_w = 67,000 g/mol in Equation (9).

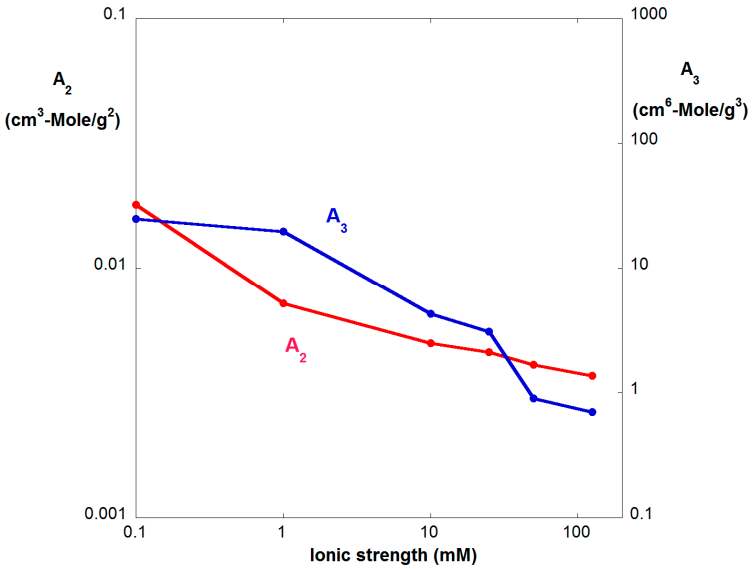

Figure 3. A_2 and A_3 vs. IS, as determined from Figure 2. The A_3 axis has two decades for each decade of the A_2 axis, suggesting an approximate correspondence to the power law between A_2 and A_3 of Equation (11) for hard spheres.

Figure 3 shows A_2 and A_3 vs. IS from these determinations. While both A_2 and A_3 follow the same expected decreasing trend vs. IS, they do not overlap using the double-y scale of Figure 3. Nonetheless, the representation which brings them into rough parity is two orders of magnitude in A_3 for each order of magnitude in A_2, which is reminiscent of the relationship between A_2 and A_3 that Boltzmann found for hard spheres [56].

$$A_3 = \frac{5MA_2{}^2}{8} \tag{11}$$

While charged, random coil polymers, which the Am/SS resemble, are not expected at all to follow hard sphere behavior the approximate scaling in Equation (11) for the data in Figure 3 is nonetheless suggestive of an underlying relationship between the two and three body interactions of the different morphologies.

Figure 4 shows $[F_{\text{inst,Am}}]$ and $[F_{\text{inst,SS}}]$ vs. C_p in the highly dilute, last stage detector train for reaction B. $[F_{\text{inst,SS}}]$ decreases as the reaction proceeds, similar to Figure 1b, which is shown in the time domain. Also shown is $I_R(90)/KC_p$ vs. C_p. Because these data are gathered in the highly diluted last stage, and under an ionic strength of 150 mM, this is a good approximation to the weight average molar mass M_w. Although there was a MALS detector in the highly dilute last stage, there was no measurable angular dependence over the M_w range produced so $I_R(90)$ is used for the M_w determination. M_w starts at around 5×10^4 g/mol and increases linearly until 50% conversion by mass, during the period that $[F_{\text{inst,SS}}]$ falls gradually, at which point it levels off, and then increases again as the SS is fully consumed in the last 10% of conversion.

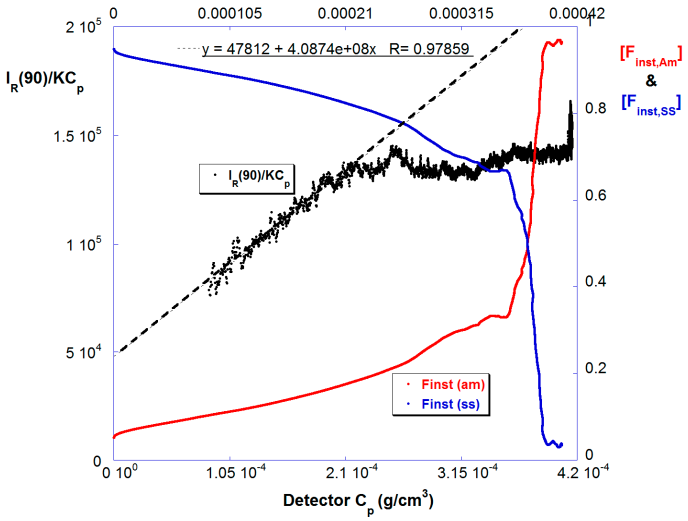

Figure 4. The instantaneous comonomer compositions $[F_{\text{inst,SS}}]$ and $[F_{\text{inst,Am}}]$ (right hand axis) and effective M_w (left hand axis) for Reaction B.

Figure 5 shows $I_R(90)$ vs. C_p in the more concentrated SGA train, for reaction B in Table 1, where C_p is the concentration of copolymer in the SGA detector train. Again, the effect of A_2 and A_3 is seen as $I_R(90)$ acquires first a negative second derivative and then a maximum.

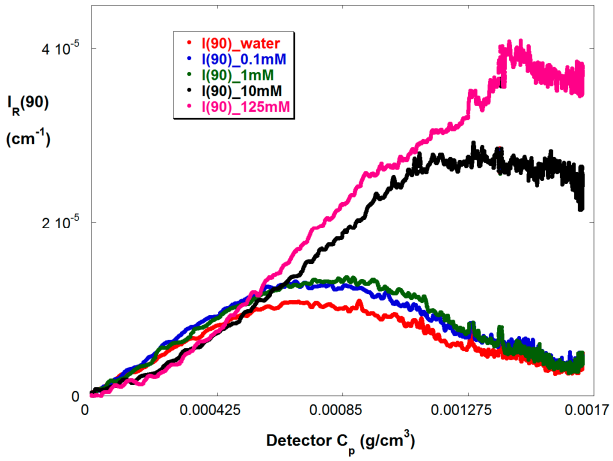

Figure 5. $I_R(90)$ at various ionic strengths for reaction B.

Figure 6 shows η_r vs. C_p in the dilute train for reaction B at five different ionic strengths. The expected trend is found that at any point in the polymerization reaction η_r decreases with increasing IS. The inset shows the final values of η_r, showing nearly a factor of four drop in η_r from low to high IS.

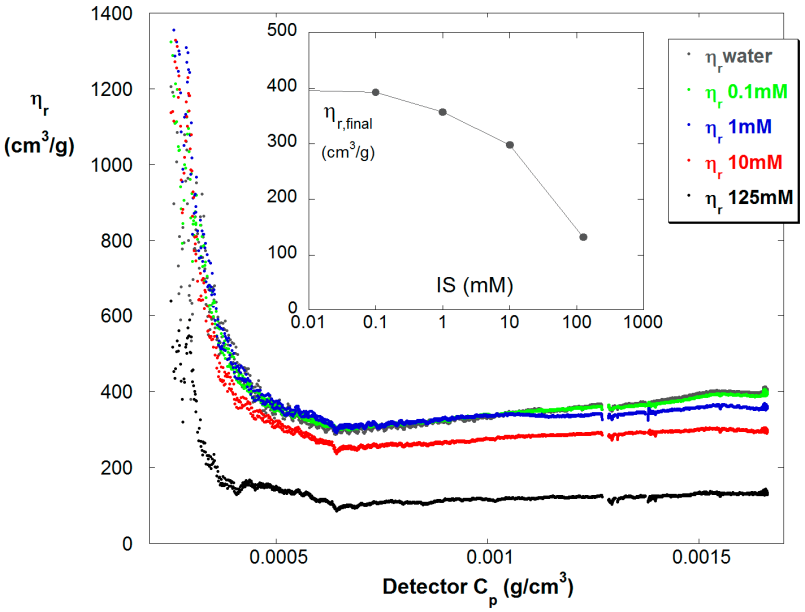

Figure 6. η_r vs. C_p at the various IS for reaction B.

4.3. Contrasting Viscosity Behavior in a Low to High ξ Reaction with a High to Low ξ Reaction

As seen in the batch reactions above, the high reactivity ratio of SS compared to Am results in rapid consumption of SS, which means the copolymer proceeds from high negative ξ which decreases to ξ = 0 once the pure polyacrylamide stage is reached during the latter portion of the reaction. A means of starting with ξ = 0 and increasing ξ = 0 during the reaction is to start with pure Am and feed in a stock of SS (a semi-batch reaction). The semi-batch reaction (reaction C) started with pure Am, had a constant flow of SS into the reactor, and ended with almost 100% SS. It was arranged so that the final polymer concentration was comparable to the final polymer concentration in the batch reaction. The molar masses are also comparable.

The specific viscosity for the batch reaction at three different IS is shown in Figure 7a. η_{sp} has a negative second derivative during the entire reaction at the three IS shown. This shows how the highly charged chains at the beginning of the reaction rapidly increase η_{sp}, but then the increase of η_{sp} slows down as the chains become less and less charged as $[F_{inst,Am}]$ increases.

In contrast Figure 7b shows a positive second derivative for η_{sp} as SS flows into the reactor. This shows how increasing ξ rapidly increases η_{sp} as $[F_{inst,SS}]$ increases. The increase in $[F_{inst,SS}]$ due to semi-batch operation of reaction C is shown in Figure 8, which can be contrasted with Figures 1b and 4 to see the opposite trends in the batch reactions A and B.

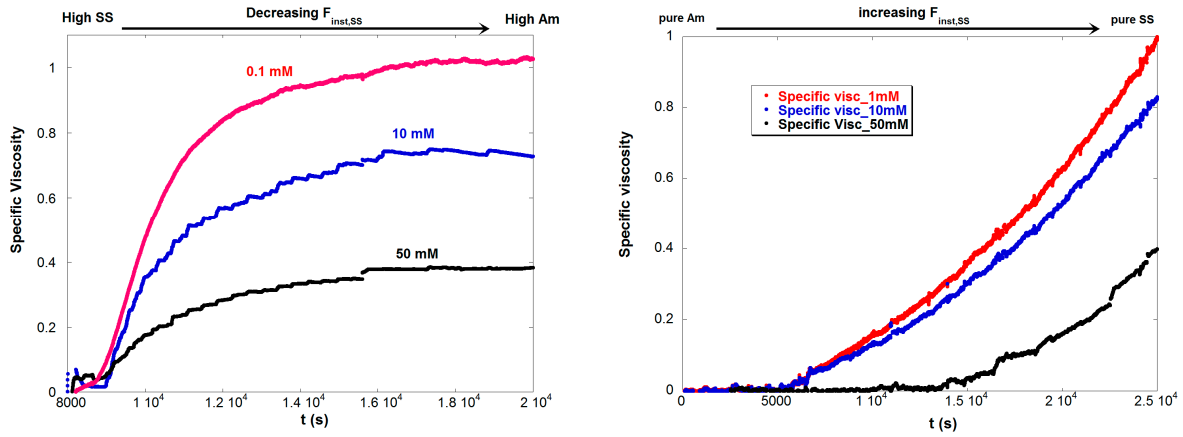

(**a**) (**b**)

Figure 7. (**a**) ν_{sp} vs. t for Reaction A, a batch reaction. The negative second derivative in time reflects the decreasing linear charge density (ξ) in the chains as the reaction proceeds. (**b**) The semi-batch Reaction C, has a positive second derivative in time, showing the effect of increasing ξ as the reaction proceeds. Both reactions ended with the same total polymer concentration.

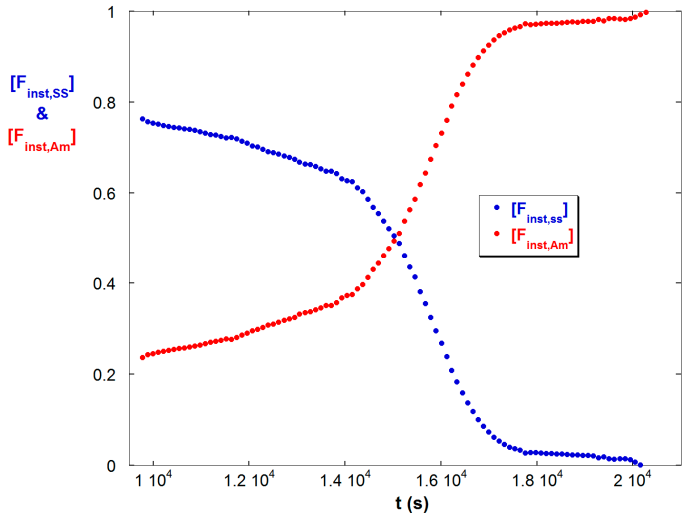

Figure 8. [$F_{inst,SS}$] and [$F_{ionst,Am}$] for the semi-batch reaction C. The trends are opposite those of batch reactions A and B.

5. Summary

A second generation ACOMP system (SGA) has been prototyped and introduced. It is capable of changing solution conditions in serial fashion on a flowing sample stream in up to seven different conditions. A detector stage, consisting of a viscometer and light scattering detector, is present in each successive sample condition, allowing the influence of several solution conditions to be monitored at each instant during the synthesis of polymers.

The first reaction used to demonstrate the capacity of the new system was the copolymerization of a neutral monomer (Am) with an anionic monomer (SS) in both batch and semi-batch processes. The difference in reactivity ratios led to high drift in composition towards chains richer in Am as reactions proceeded, corresponding to lower linear charge density ξ. The effects of up to seven different ionic strengths on reduced viscosity and the virial coefficients A_2 and A_3 were monitored for batch and semi-batch reactions. The A_2 and A_3 effects, monitored by light scattering, were pronounced

at low IS, leading to maxima in scattering during the reaction which then subsided as the reaction progressed further. These strong interparticle effects were largely screened and minimized at high IS. The behavior of reduced viscosity followed the expected trend of decreasing with increasing IS at all points during the reaction. When a semi-batch reaction was run such that SS was increased, and hence also ξ, η_r increased with a positive second derivative in time, whereas a batch reaction with similar concentrations led to a negative second derivative in time due to ξ decreasing in time.

The SGA should be useful for reactions where stimuli responsive polymers are produced. These include living type copolymerization of block copolymers which exhibit an LCST, and those which can micellize and entrap substances, such as drugs. It may also be possible to develop formulations, since different agents can be added in the seven solution condition system.

It is noted that APMT, Inc. has implemented first generation ACOMP on industrial scale reactors. Hence, scale-up of SG-ACOMP is expected to follow a similar path. It is hoped that, as stimuli responsive polymers become a larger part of the polymer manufacturing sector, SG-ACOMP, or similar, can be integrated into plant design. Similarly, the active, automatic control of conventional polymer synthesis [50] is currently being adapted for living type reactions, on which the synthesis of many stimuli responsive polymers relies.

Acknowledgments: This work was supported by NSF EPS-1430280 and Louisiana Board of Regents.

Author Contributions: Aide Wu improved the instrumentation and carried out most of the experiments. Michael F. Drenski contributed to the design and build of the original SGA system and guided many of the improvements. Zifu Zhu helped build the original SGA system, together with Michael F. Drenski, and carried out the semi-batch reaction and reaction A in the work. Wayne F. Reed conceived the idea of SG-ACOMP and the multiple syringe pump approach to changing conditions in serial flow, and wrote most of this manuscript.

Conflicts of Interest: The authors declare no conflict of interest.

References

1. Zhuang, J.; Gordon, M.R.; Ventura, J.; Li, L.; Thayumanavan, S. Multi-stimuli responsive macromolecules and their assemblies. *Chem. Soc. Rev.* **2013**, *42*, 7421–7435. [CrossRef] [PubMed]
2. Jeong, B.; Gutowska, A. Lessons from nature: Stimuli-responsive polymers and their biomedical applications. *Trends Biotechnol.* **2002**, *20*, 305–311. [CrossRef]
3. Nath, N.; Chilkoti, A. Creating "smart" surfaces using stimuli responsive polymers. *Adv. Mater.* **2002**, *14*, 1243–1247. [CrossRef]
4. Liu, F.; Urban, M.W. Recent advances and challenges in designing stimuli-responsive polymers. *Prog. Polym. Sci.* **2010**, *35*, 3–23. [CrossRef]
5. Galaev, I.; Mattiasson, B. *Smart Polymers: Applications in Biotechnology and Biomedicine*; CRC Press: Boca Raton, FL, USA, 2007.
6. Chung, J.E.; Yokoyama, M.; Yamato, M.; Aoyagi, T.; Sakurai, Y.; Okano, T. Thermo-responsive drug delivery from polymeric micelles constructed using block copolymers of poly(*n*-isopropylacrylamide) and poly(butylmethacrylate). *J. Control. Release* **1999**, *62*, 115–127. [CrossRef]
7. Zhang, J.; Peppas, N.A. Synthesis and characterization of pH-and temperature-sensitive poly(methacrylic acid)/poly(*n*-isopropylacrylamide) interpenetrating polymeric networks. *Macromolecules* **2000**, *33*, 102–107. [CrossRef]
8. Jain, S.; Bates, F.S. On the origins of morphological complexity in block copolymer surfactants. *Science* **2003**, *300*, 460–464. [CrossRef] [PubMed]
9. Matyjaszewski, K.; Sumerlin, B.S.; Tsarevsky, N.V.; Chiefari, J. *Controlled Radical Polymerization*; American Chemical Society: Washington, DC, USA, 2016.
10. Ballard, N.; Mecerreyes, D.; Asua, J.M. Redox active compounds in controlled radical polymerization and dye-sensitized solar cells: Mutual solutions to disparate problems. *Chem. A Eur. J.* **2015**, *21*, 18516–18527. [CrossRef] [PubMed]
11. Mastan, E.; Li, X.; Zhu, S. Modeling and theoretical development in controlled radical polymerization. *Prog. Polym. Sci.* **2015**, *45*, 71–101. [CrossRef]

12. Chan, N.; Cunningham, M.F.; Hutchinson, R.A. Copper-mediated controlled radical polymerization in continuous flow processes: Synergy between polymer reaction engineering and innovative chemistry. *J. Polym. Sci. Part A Polym. Chem.* **2013**, *51*, 3081–3096. [CrossRef]
13. Barner-Kowollik, C.; Delaittre, G.; Gruendling, T.; Paulöhrl, T. Elucidation of reaction mechanisms and polymer structure: Living/controlled radical polymerization. In *Mass Spectrometry in Polymer Chemistry*; Wiley-VCH Verlag GmbH & Co. KGaA: Weinheim, Germany, 2011; pp. 373–403.
14. Flores, J.D.; Abel, B.A.; Smith, D.; McCormick, C.L. Stimuli-responsive polymers via controlled radical polymerization. In *Monitoring Polymerization Reactions*; John Wiley & Sons: New York, NY, USA, 2013; pp. 45–58.
15. Hemp, S.T.; Long, T.E. DNA-inspired hierarchical polymer design: Electrostatics and hydrogen bonding in concert. *Macromol. Biosci.* **2012**, *12*, 29–39. [CrossRef] [PubMed]
16. Cheng, S.; Zhang, M.; Dixit, N.; Moore, R.B.; Long, T.E. Nucleobase self-assembly in supramolecular adhesives. *Macromolecules* **2012**, *45*, 805–812. [CrossRef]
17. Roy, R.K.; Meszynska, A.; Laure, C.; Charles, L.; Verchin, C.; Lutz, J.-F. Design and synthesis of digitally encoded polymers that can be decoded and erased. *Nat. Commun.* **2015**, *6*, 7237. [CrossRef] [PubMed]
18. Lutz, J.-F.; Ouchi, M.; Liu, D.R.; Sawamoto, M. Sequence-controlled polymers. *Science* **2013**, *341*, 1238149. [CrossRef] [PubMed]
19. Landau, L.D.; Lifshitz, E.M. *Statistical Physics*, 3rd ed.; Pergammon Press: Oxford, UK; New York, NY, USA, 1980.
20. Flory, P.J. *Principles of Polymer Chemistry*; Cornell University Press: New York, NY, USA, 1953.
21. Yamakawa, H. *Modern Theory of Polymer Solutions*; Harper & Row: New York, NY, USA, 1971.
22. McMillan, W.G., Jr.; Mayer, J.E. The statistical thermodynamics of multicomponent systems. *J. Chem. Phys.* **1945**, *13*, 276–305. [CrossRef]
23. Hansen, J.-P.; McDonald, I.R. *Theory of Simple Liquids*; Elsevier: Amsterdam, The Netherlands, 1990.
24. Odijk, T. Polyelectrolytes near the rod limit. *J. Polymer Sci. Polym. Phys. Ed.* **1977**, *15*, 477–483. [CrossRef]
25. Skolnick, J.; Fixman, M. Electrostatic persistence length of a wormlike polyelectrolyte. *Macromolecules* **1977**, *10*, 944–948. [CrossRef]
26. Sorci, G.A.; Reed, W.F. Electrostatically enhanced second and third virial coefficients, viscosity, and interparticle correlations for linear polyelectrolytes. *Macromolecules* **2002**, *35*, 5218–5227. [CrossRef]
27. Reed, W.; Ghosh, S.; Medjahdi, G.; Francois, J. Dependence of polyelectrolyte apparent persistence lengths, viscosity, and diffusion on ionic strength and linear charge density. *Macromolecules* **1991**, *24*, 6189–6198. [CrossRef]
28. Manning, G.S. Limiting laws and counterion condensation in polyelectrolyte solutions II. Self-diffusion of the small ions. *J. Chem. Phys.* **1969**, *51*, 934–938. [CrossRef]
29. Oosawa, F. *Polyelectrolytes*; Marcel Dekker Inc.: New York, NY, USA, 1971.
30. Wilson, R.W.; Bloomfield, V.A. Counterion-induced condesation of deoxyribonucleic acid. A light-scattering study. *Biochemistry* **1979**, *18*, 2192–2196. [CrossRef] [PubMed]
31. Hinderberger, D.; Spiess, H.W.; Jeschke, G. Dynamics, site binding, and distribution of counterions in polyelectrolyte solutions studied by electron paramagnetic resonance spectroscopy. *J. Phys. Chem. B* **2004**, *108*, 3698–3704. [CrossRef]
32. Kreft, T.; Reed, W.F. Experimental observation of crossover from noncondensed to counterion condensed regimes during free radical polyelectrolyte copolymerization under high-composition drift conditions. *J. Phys. Chem. B* **2009**, *113*, 8303–8309. [CrossRef] [PubMed]
33. Mayo, F.R.; Lewis, F.M. Copolymerization. I. A basis for comparing the behavior of monomers in copolymerization; the copolymerization of styrene and methyl methacrylate. *J. Am. Chem. Soc.* **1944**, *66*, 1594–1601. [CrossRef]
34. Kreft, T.; Reed, W.F. Predictive control of average composition and molecular weight distributions in semibatch free radical copolymerization reactions. *Macromolecules* **2009**, *42*, 5558–5565. [CrossRef]
35. Florenzano, F.H.; Strelitzki, R.; Reed, W.F. Absolute, on-line monitoring of molar mass during polymerization reactions. *Macromolecules* **1998**, *31*, 7226–7238. [CrossRef]
36. Reed, W.F. Automated continuous online monitoring of polymerization reactions (acomp) and related techniques. In *Encyclopedia of Analytical Chemistry*; John Wiley & Sons, Ltd.: New York, NY, USA, 2006.

37. Çatalgil-Giz, H.; Giz, A.; Alb, A.M.; Öncül Koç, A.; Reed, W.F. Online monitoring of composition, sequence length, and molecular weight distributions during free radical copolymerization, and subsequent determination of reactivity ratios. *Macromolecules* **2002**, *35*, 6557–6571. [CrossRef]
38. Alb, A.M.; Enohnyaket, P.; Drenski, M.F.; Head, A.; Reed, A.W.; Reed, W.F. Online monitoring of copolymerization involving comonomers of similar spectral characteristics. *Macromolecules* **2006**, *39*, 5705–5713. [CrossRef]
39. Alb, A.M.; Paril, A.; Catalfil-Giz, H.; Giz, A.; Reed, W.F. Evolution of composition, molar mass, and conductivity during the free radical copolymerization or polyelectrolytes. *J. Phys. Chem. B* **2007**, *111*, 8560–8566. [CrossRef] [PubMed]
40. Farinato, R.S.; Calbick, J.; Sorci, G.A.; Florenzano, F.H.; Reed, W.F. Online monitoring of the final, divergent growth phase in the step-growth polymerization of polyamines. *Macromolecules* **2005**, *38*, 1148–1158. [CrossRef]
41. Alb, A.M.; Reed, W.F. Simultaneous monitoring of polymer and particle characteristics during emulsion polymerization. *Macromolecules* **2008**, *41*, 2406–2414. [CrossRef]
42. Alb, A.M.; Farinato, R.; Calbick, J.; Reed, W.F. Online monitoring of polymerization reactions in inverse emulsions. *Langmuir* **2006**, *22*, 831–840. [CrossRef] [PubMed]
43. Kreft, T.; Reed, W.F. Predictive control and verification of conversion kinetics and polymer molecular weight in semi-batch free radical homopolymer reactions. *Eur. Polym. J.* **2009**, *45*, 2288–2303. [CrossRef]
44. Grassl, B.; Reed, W.F. Online polymerization monitoring in a continuous reactor. *Macromol. Chem. Phys.* **2002**, *203*, 586–597. [CrossRef]
45. Paril, A.; Alb, A.M.; Reed, W.F. Online monitoring of the evolution of polyelectrolyte characteristics during postpolymerization modification processes. *Macromolecules* **2007**, *40*, 4409–4413. [CrossRef]
46. Mignard, E.; Leblanc, T.; Bertin, D.; Guerret, O.; Reed, W.F. Online monitoring of controlled radical polymerization: Nitroxide-mediated gradient copolymerization. *Macromolecules* **2004**, *37*, 966–975. [CrossRef]
47. Mignard, E.; Lutz, J.-F.; Leblanc, T.; Matyjaszewski, K.; Guerret, O.; Reed, W.F. Kinetics and molar mass evolution during atom transfer radical polymerization of *n*-butyl acrylate using automatic continuous online monitoring. *Macromolecules* **2005**, *38*, 9556–9563. [CrossRef]
48. Alb, A.M.; Serelis, A.K.; Reed, W.F. Kinetic trends in raft homopolymerization from online monitoring. *Macromolecules* **2008**, *41*, 332–338. [CrossRef]
49. Alb, A.M.; Enohnyaket, P.; Craymer, J.F.; Eren, T.; Coughlin, E.B.; Reed, W.F. Online monitoring of ring-opening metathesis polymerization of cyclooctadiene and a functionalized norbornene. *Macromolecules* **2007**, *40*, 444–451. [CrossRef]
50. McAfee, T.; Leonardi, N.; Montgomery, R.; Siqueira, J.; Zekoski, T.; Drenski, M.F.; Reed, W.F. Automatic control of polymer molecular weight during synthesis. *Macromolecules* **2016**, *49*, 7170–7183. [CrossRef]
51. Alb, A.M.; Drenski, M.F.; Reed, W.F. Simultaneous continuous, nonchromatographic monitoring and discrete chromatographic monitoring of polymerization reactions. *J. Appl. Polym. Sci.* **2009**, *113*, 190–198. [CrossRef]
52. McFaul, C.A.; Alb, A.M.; Drenski, M.F.; Reed, W.F. Simultaneous multiple sample light scattering detection of LCST during copolymer synthesis. *Polymer* **2011**, *52*, 4825–4833. [CrossRef]
53. McFaul, C.A.; Drenski, M.F.; Reed, W.F. Online, continuous monitoring of the sensitivity of the LCST of nipam-Am copolymers to discrete and broad composition distributions. *Polymer* **2014**, *55*, 4899–4907. [CrossRef]
54. Huggins, M.L. The viscosity of dilute solutions of long-chain molecules. *J. Am. Chem. Soc.* **1942**, *64*, 2716–2718. [CrossRef]
55. Zimm, B.; Stein, R.; Doty, P. Polymer bull. 1 (1945) 90; bh zimm. *J. Chem. Phys.* **1948**, *16*, 1093. [CrossRef]
56. Hansen, J.P.; McDonald, I.R. *Theory of Simple Liquids*; Acdamic Press: New York, NY, USA, 1986.